SUPPORTING INFORMATION

Highly Stable and Efficient Inverted Organic Solar Cells Based on Low-Temperature Solution-Processed PEIE and ZnO Bilayers

Won-Yong Jin,[a] Riski Titian Ginting,[a] Sung-Ho Jin,[b] and Jae-Wook Kang [a]*

[a]Department of Flexible and Printable Electronics, Polymer Materials Fusion Research Center, Chonbuk National University, Jeonju 54896, Korea.

Email: jwkang@jbnu.ac.kr

[b]Department of Chemistry Education, Graduate Department of Chemical Materials, Institute for Plastic Information and Energy Materials, Pusan National University, Busan 46241 Korea.

Email: shjin@pusan.ac.kr

W.-Y and R.T. contributed equally to this work.

Survey-scan XPS

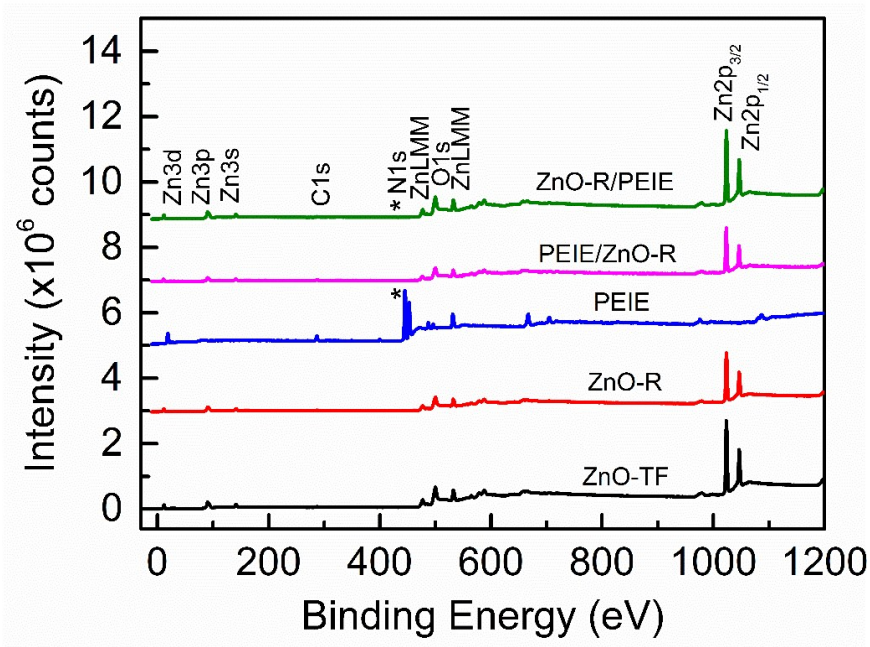

Figure S1. Survey scan of various interlayer configurations.

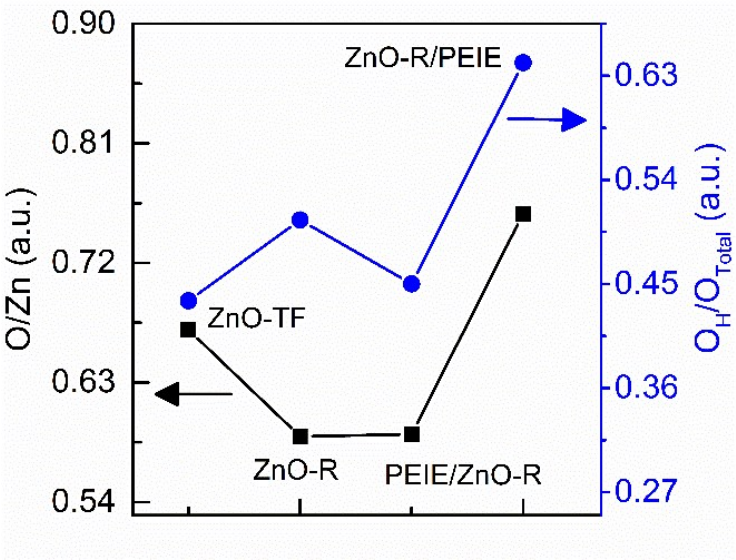

Figure S2. Oxygen (O) to zinc (Zn) ratio and the relative quantities of oxygen defects (O_H/O_{Total}) for various ETL configurations.

Surface Topography

AFM surface topography images of ZnO-TF, ZnO-R, PEIE, ZnO-R/PEIE, and PEIE/ZnO-R films are presented in Figure S3. The ZnO-R sample revealed a significantly high root mean square (RMS) roughness of about 10.2 nm and a distinct rippled structure with a peak height of about 20 nm. By contrast, the ZnO-TF and PEIE films on ITO exhibited relatively smooth surfaces with RMS roughnesses of approximately 2.5 nm and 2.3 nm, respectively. The introduction of a PEIE layer between ITO and ZnO-R did not change the RMS roughness, as shown in Figure 3(d). However, the RMS roughness of the ZnO-R/PEIE film increased slightly from 10.2 nm to 12.3 nm.

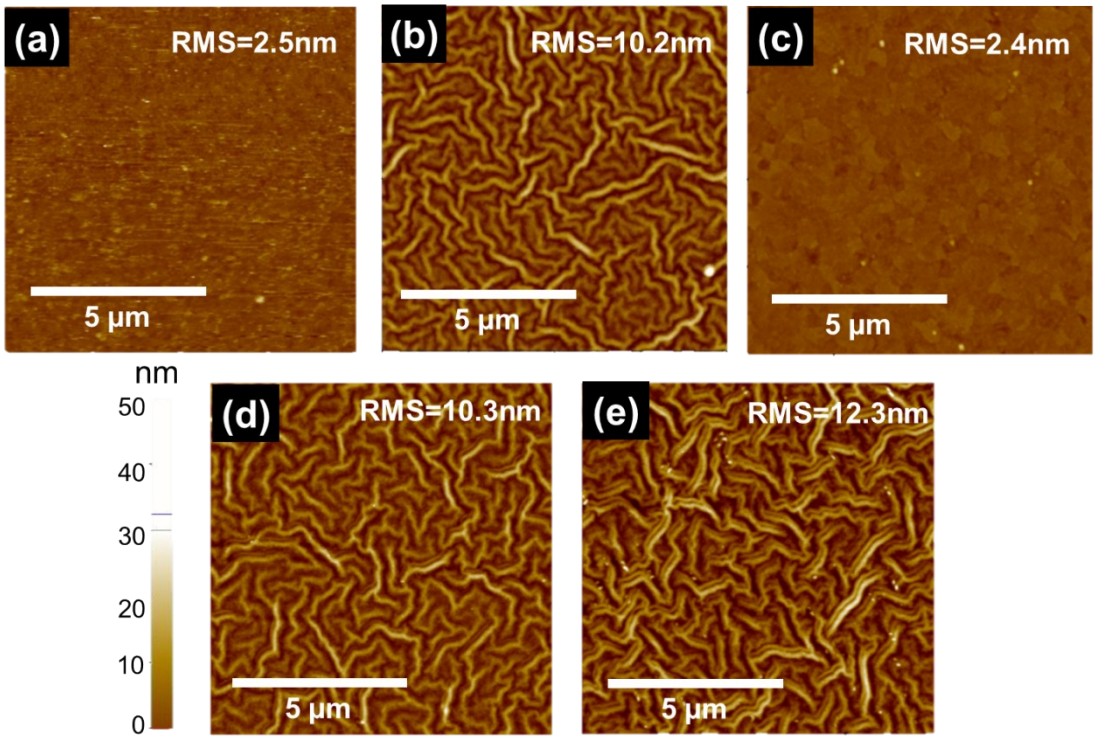

Figure S3. AFM topography images (10×10 μm) of (a) ZnO-TF, (b) ZnO-R, (c) PEIE, (d) PEIE/ZnO-R, and (e) ZnO-R/PEIE layers on ITO substrates.

Photoluminescence measurement

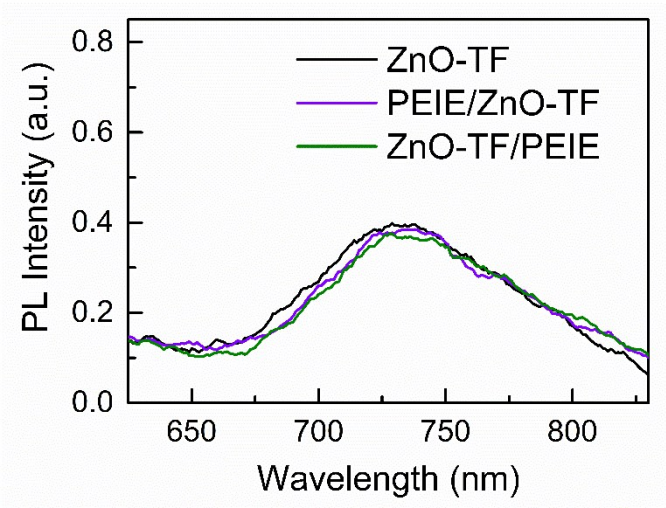

Fig. S4. PL spectra of PTB7:$PC_{71}BM$ coated on different structure of ZnO-TF, PEIE/ZnO-TF, and ZnO-TF/PEIE

Dark J-V Characteristics

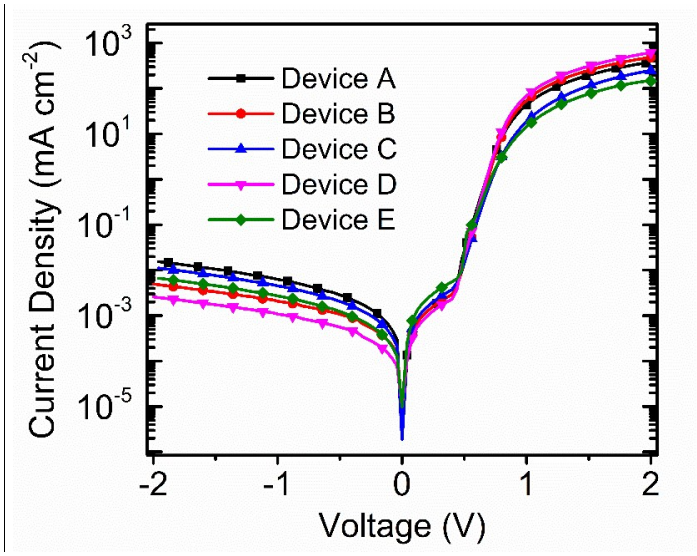

Figure S5. Dark J-V curves for various device configuration.

Reflectance measurement

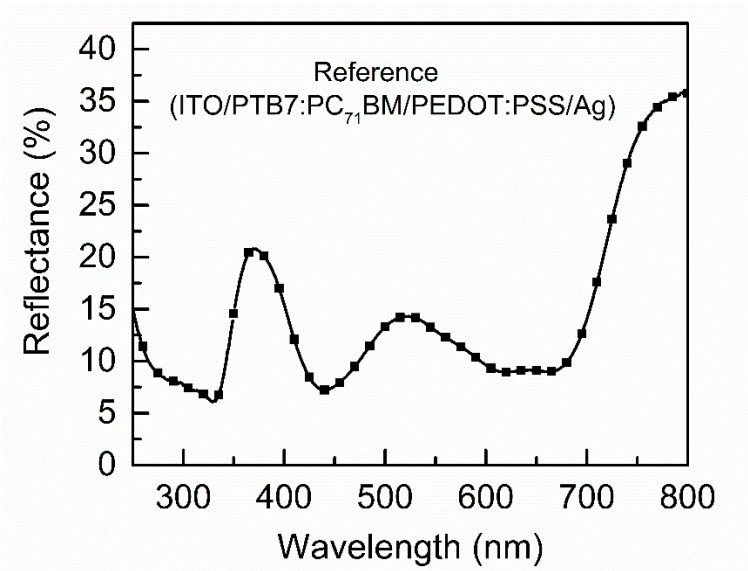

Figure S6. Reflectance spectrum of reference device without ETL.

Photo-CELIV measurement

In the present configuration, a blue laser (473 nm) was employed to illuminate devices through the ITO electrode, where bias and offset voltages are applied. To avoid marginal errors in mobility approximations due to space charge effects and charge recombination processes,[1] a reduced laser power of less than 0.05 μJ cm^{-2} was utilized with the objective of maintaining an *n* value of less than 10^{17} cm^{-3}. Charge carrier mobilities were calculated using a modified equation to determine the true charge mobility, even under high charge density conditions ($\Delta j/j_0 < 0.95$).[1] As described in a prior report, the photo-generated charge carrier concentration was computed by integrating the conduction current over the extraction time.[2] Furthermore, the electric field was defined as $E = 0.65 * A t_{max}/d$, where A is the voltage slope, t_{max} is the time required for the transient current to reach a maximum value, and d is the total distance between the anode and cathode. This expression more accurately represented non-constant electric fields during current extraction.[1] For all devices, $\Delta j/j_0$ was calculated to be less than 0.50.

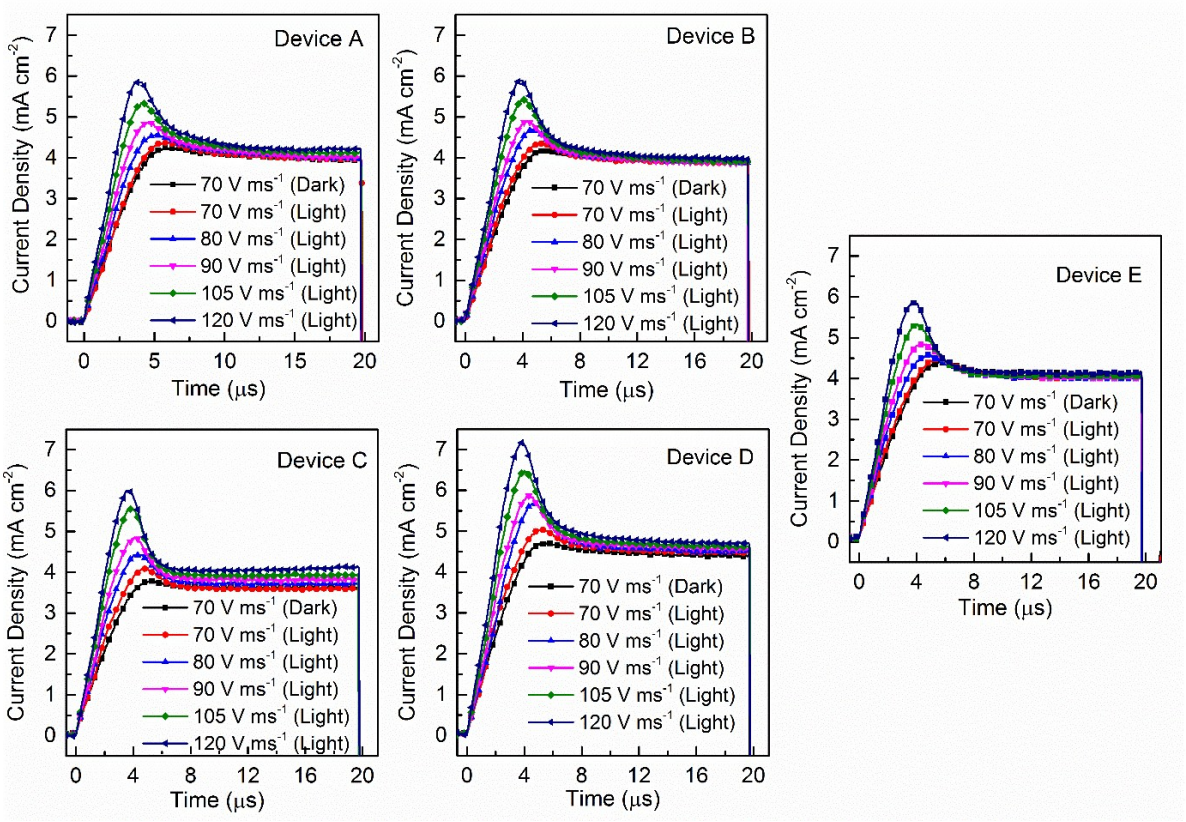

Figure S7. Photo-CELIV transients of various device configurations under different applied electric field at constant laser intensity of ≤ 0.05 μJ/cm

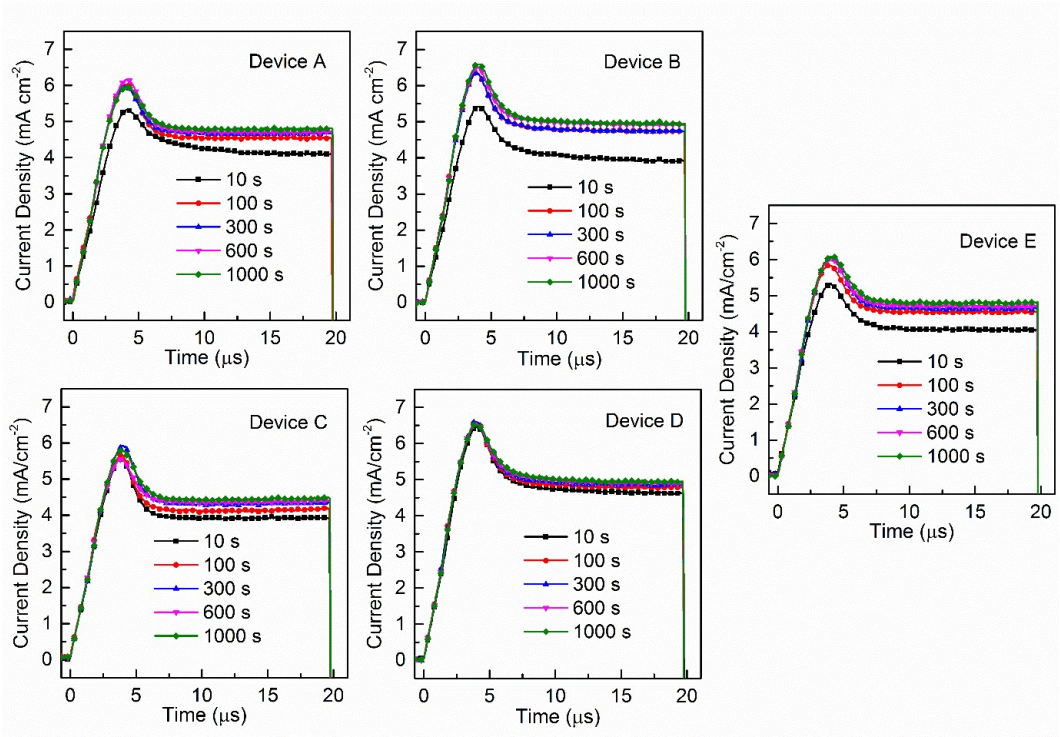

Figure S8. Photo-CELIV transients of various device configurations with different light soaking duration (1 Sun condition) at constant laser intensity of 0.05 μJ/cm^2.

References

1 S. Bange, M. Schubert and D. Neher, *Phys. Rev. B*, 2010, **81**, 035209.

2 B. Homa, M. Andersson and O. Inganäs, *Org. Electron.*, 2009, **10**, 501-505.